Received: 6 April 2022 | Revised: 2 June 2022 | Accepted: 6 June 2022

DOI: 10.1002/apj.2807

RESEARCH ARTICLE

Asia-Pacific Journal of Chemical Engineering | Curtin University | WILEY

Experimental research on fully burning high-alkali coal in a 300 MW boiler with slag-tap furnace

Yuguo Ni[1] | Shihao Hu[1] | Hanxiao Meng[1] | Jiankang Wang[1] | Hui Li[1,2] | Hao Zhou[3] | Xiang Ma[4] | Hao Zhou[1]

[1]State Key Laboratory of Clean Energy Utilization, Institute for Thermal Power Engineering, Zhejiang University, Hangzhou, China

[2]China Huaneng Group CO, LTD, Beijing, China

[3]Tianjin Huaneng Yanliuqing Power CO, LTD, Tianjin, China

[4]Xi'an Thermal Power Research Institute CO, LTD, Xi'an, China

Correspondence
Hao Zhou, Zhejiang University, State Key Laboratory of Clean Energy Utilization, Institute for Thermal Power Engineering, Hangzhou 310027, China.
Email: zhouhao@zju.edu.cn

Funding information
National Key Research & Development Program of China, Grant/Award Number: 2018YFB0604104

Abstract

Safety issues such as contamination and slagging restrict the use of high-alkali coal. To explore the possibility of fully burning high-alkali coal in a boiler with slag-tap furnace, Na_2CO_3-blended burning tests and a fully burning high-alkali coal test were carried out in a 300 MW boiler with slag-tap furnace. The results showed that fully burning high-alkali coal had little effect on the steam parameters and the boiler could operate safely. The Na content in the flue gas tended to decrease from SH5 to RH2 and increased from RH2 to ECON. The increase of Na content in the fuel would significantly raise Na content in the flue gas, slightly increase the K content, and increase the ability of liquid slag to capture Na. Before the Na content in SH coal ash was increased by 150%, the capture ability of liquid slag to Na had reached saturation. The added Na_2CO_3 made the Al and Ca elements migrate to the liquid slag to form a high melting point Na-Al-Ca compound. The microstructure analysis showed that liquid slag has a rich pore structure inside and outside and the Na content in the pore was higher than that out. Mineralogy analysis found that deposition samples mainly included Quartz, Magnesioferrite, Anhydrite, Lime, and $CaSiO_4$ and the addition of Na_2CO_3 hardly affected the mineral composition.

KEYWORDS

alkali metals, boiler with slag-tap furnace, high-alkali coal, Na_2CO_3

1 | INTRODUCTION

Clean energy lights the road for the future development direction of the electric power industry. Although the Chinese government has issued a series of policies to encourage the development of clean energy, the dominant position of coal in China's energy structure will not change in the short term. Coal power accounts for 60.70% of China's annual energy generation capacity in 2020, with hydropower at 17.77%, wind power at 6.12%, nuclear power at 4.80%, and solar power at 3.42%.[1] And coal power plays the role of "pillar" and "ballast" to ensure a safe and stable electricity supply. The safe, efficient, and high-economic operation of existing power plants is essential. High-alkali coal in Xinjiang has the advantages of high burnout, low ash content, and low cost, which is suitable for power generation and has enormous reserves. It is estimated that there are 390 billion tons of Zhundong coal[2] and 570.8 billion tons of Hami coal.[3] The shallow burial depth makes its development value great.[2,4] High-alkali coal has a large reserve and great advantages in combustion characteristics. Suppose it is possible to fully burn high-alkali coal and build a corresponding power plant in the coal districts. The energy shortage problem can be greatly alleviated, and a long-term energy supply can be guaranteed in China.

When high-alkali coal is burned in existing power plants, however, the heat transfer surface suffers from severe contamination and slagging, resulting in large-scale accidents such as tube overheating and bursting, jeopardizing the boiler's safety.

Domestic and foreign researchers have carried out a lot of research on the contamination mechanism[5,6] and prevention of contamination and slagging[7,8] to realize the full combustion of high-alkali coal. Wang et al.[9] analyzed the slags/deposits of a 350 MW boiler fully burning high-alkali coal and found that the condensation and deposition of sodium and calcium sulfates played an essential role in ash deposition on the heat transfer surfaces. Li et al.[5] studied the formation of fine particles and the deposition of ash during the combustion of high-sodium Zhundong coal. They found that in the initial stage of fouling, small particles with high adhesion play a leading role for large ash particles that will quickly rebound after hitting the tube. And in the later stage, the alkali and alkaline earth metal elements (AAEMs) in the Zhundong coal can enhance the viscosity of ash particles. And the fine sticky particles rich in Na, Ca, Cl, and S can enhance ash deposition. Li et al.[10] found that the ash deposited on the heat transfer surface will react with the Na in the flue gas at high temperature and increase the Na content in the deposition, resulting in more severe contamination. Kaolin, rich in SiO_2 and Al_2O_3, has a large specific surface area and plenty of pore structure. It has a good chemical adsorption effect on sodium and is considered the best additive to inhibit high-alkali coal contamination and slagging.[7] Dou et al.,[11] Dai et al.,[12] and Low et al.[13] found that kaolin can capture gaseous sodium in the flue gas by forming high melting silicate or aluminosilicate substances. Zhang et al.[14] found that the silica-alumina minerals in the coal ash can capture sodium and reduce the sodium releasing rate. But calcium will weaken this capture effect. And the sodium release rate is related to the mole fraction ratio of (Ca + Mg)/(Al + Si). Zhou et al.[8] applied a new method, namely, intercalationexfoliation combined with acid leaching, to improve the capture efficiency of kaolin and found that kaolin modified displays a better sodium capture performance. Besides, studies by Nielsen et al.[15] and Mayoral et al.[16] have shown that the oxidizing combustion atmosphere could effectively control the contamination and slagging caused by Na sublimation. Based on these studies, scholars tried to fully burn high-alkali coal. But even if the boiler is designed for fully burning high-alkali coal, the proportion of high-alkali coal is generally between 70% and 80%,[17,18] which cannot meet the requirements for fully burning high-alkali coal. Lan et al.[19] and Li et al.[20] proposed fully burning high-alkali coal in a boiler with slag-tap furnace. Lan et al.[19] found that adopting the liquid slag discharge in the horizontal cyclone furnace can effectively improve the capture capacity of the liquid slag to Na and K. The capture efficiency can reach more than 50%. Zhou et al.[21] carried out a Zhundong coal combustion experiment on a liquid slag discharge cyclone furnace and found that the cyclone furnace has a high combustion efficiency, a high slag capture rate, and low fly ash share. But the concentration of Na and Ca in flue gas increases for the small particle size of fly ash.

The combustion technology of the boiler with slag-tap furnace has the characteristics of high combustion temperature and high combustion intensity. This combustion technology can generate a large amount of liquid slag, greatly improve the slag capture efficiency in the furnace, reduce the fly ash concentration of the flue gas at the furnace outlet, and result in a less fly ash share. Meanwhile, the heterogeneous reaction between high-temperature slag and alkali metals during the combustion process can realize the capture of Na, K, Ca, and Fe, which effectively solves the problem of slagging and contamination when burning high-alkali coal.[22,23] It is a fascinating method for fully burning high-alkali coal in a boiler with slag-tap furnace. Fully burning high-alkali coal tests were conducted on a small-scale liquid slag discharge test bench, but few studies forced on a large-scale boiler. In this work, the Na_2CO_3 mixed burning tests and a fully burning high-alkali coal test were carried out in a 300 MW boiler with slag-tap furnace to explore the possibility of fully burning high-alkali coal in a liquid slagging boiler. A self-made probe was used to collect the deposition in the boiler. The liquid slag and the fly ash were sampled. The migration properties of elements were studied. X-Ray Fluorescence (XRF), X-ray diffraction (XRD), Scanning Electron Microscope (SEM), and Energy Dispersive Spectrometer (EDS) were used to analyze the samples.

2 | EXPERIMENTAL DETAILS

2.1 | Experimental system

The experiment was conducted in a 300 MW boiler with slag-tap furnace in Tianjin, China. The boiler is subcritical, primary reheat, dual-combustor, W-shaped flame, 100% fly ash reburning, liquid slag discharge, and the tower once-through boiler with the direct-firing pulverizing system. In addition, it is arranged with two slag chambers symmetrically, one burning-out chamber and one vertical flue to form a double U-shaped boiler framework and tower structure. Eight low-NO_x swirl burners are arranged in double rows and staggered on the top of each slag chamber. After passing the furnace slag screen, high-temperature flue gas turns into the burning-out

chamber, rises into the vertical flue, and then flows through a five-stage superheater, two-stage reheater, and economizer in turn. Then, the flue turns downwards. After denitrification, rotary air heater preheating, electric precipitation, and desulfurization, the flue gas is emitted to the atmosphere. Part of the slag in the slag chamber forms liquid slag for the high temperature and is collected at the bottom of the slag chamber, then enters the slag bath through the slag discharge port, and finally picked up by the slag conveyor. The direct-firing pulverizing system consists of four volumetric coal feeders and four MPS medium speed mills. Figure 1 is the schematic diagram of the boiler and the distribution of measuring points. Four measuring points in the experiment were arranged at the middle soot blower hole before the fifth superheater (SH5), the secondary reheater (RH2), the primary reheater (RH1), and the economizer (ECON).

The deposition collection system used in the experiment consisted of a probe, a probe holder, a horizontal sliding guide rail, an oil circulation cooling system, and a data acquisition system, as shown in Figure 2. The probe was fixed on the probe holder, which could horizontally move on the sliding guide rail. An oil circulation cooling system was jointed to the probe to control the surface temperature of the probe head by the thermal conductive oil, and the oil circulation cooling system was connected to cooling water to cool the thermal conductive oil. Two K-type thermocouples were fixed inside the probe head to monitor the surface temperature, while a K-type thermocouple was fixed outside to measure the flue gas temperature. The temperature data were recorded by the data acquisition system and displayed on the computer. The temperature data of the outer thermocouple were used as probe head surface temperature. During the experiment, thermal conductive oil temperature was controlled to maintain probe head surface temperature at about 175°C, ensuring that sodium vapor in the flue gas could condense on the probe surface. The soot blower hole was covered with a plate after the probe was pushed into the furnace to prevent cold air from entering the furnace. Figure 3 is the test site picture of the deposition collection system.

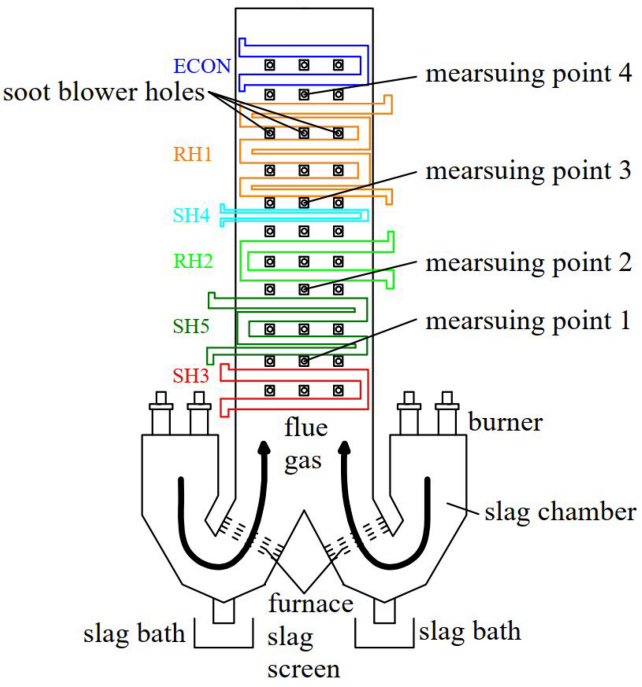

FIGURE 1 Schematic diagram of boiler and the distribution of measuring points

Figure 4 shows the structure of the probe used in the experiment. The total length of the probe was 2.5 m. The probe head was a deposition surface, with a length of 76 mm and a diameter of 40 mm, which was drilled with two holes for inserting K-type thermocouples. After the boiler ran stably, it pushed the probe horizontally into the soot blower hole. About 1.5 m of the probe was extended into the furnace and deposited about 45 min. Then, the probe was pushed out when the test was over. Finally, the deposition was collected from the probe surface. Four probes were deposited imultaneously, and samples were collected three times in each condition. Besides, fly ash was sampled before the denitrification system and after the economizer, and liquid slag (LS) was sampled before it flowed into the slag bath. To avoid interference, soot blowing was stopped during the test. All samples at six locations (LS, SH5, RH2, RH1, ECON, and fly ash) were analyzed by XRF, SEM, and XRD. Figure 5 is a picture of ash deposition on the probe head.

2.2 | Experimental conditions

Shenhua (SH) coal and Hami (HM) coal were chosen as the test coals. SHc was typical coal in the power plant. Coal properties are shown in Table 1. The chemical composition of the coal ash is shown in Table 2. The experiment included a blank group (SHc) and three experimental groups: doped with 2.5% Na_2CO_3 (2.5%Na), doped with 4% Na_2CO_3 (4%Na), and fully burnt high-alkali coal (HMc). Among four conditions, both slag chambers of the SHc condition burnt SH coal. For 2.5% Na and 4%Na conditions, to ensure the safe operation of the boiler and avoid security risks caused by direct burning of high-alkali coal, the Na content in the coal ash was increased to 2.5% and 4% to simulate high-alkali coal by adding Na_2CO_3 to SH coal. To ensure that Na_2CO_3 and coal were fully contacted and evenly mixed, Na_2CO_3 was stably added to the coal bunker through the feeder when

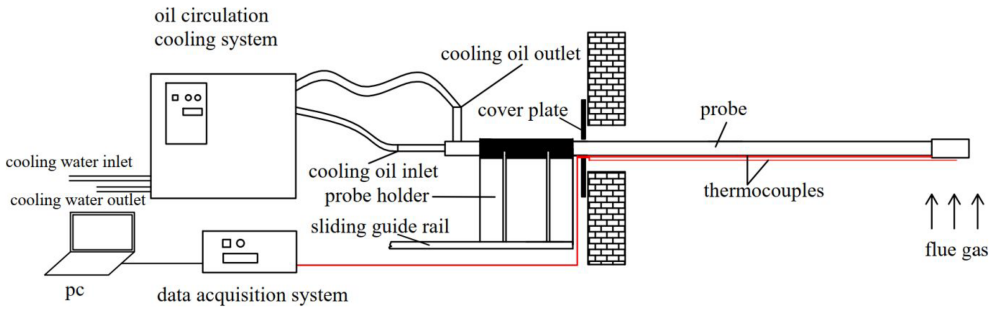

FIGURE 2 Schematic diagram of the deposition collection system

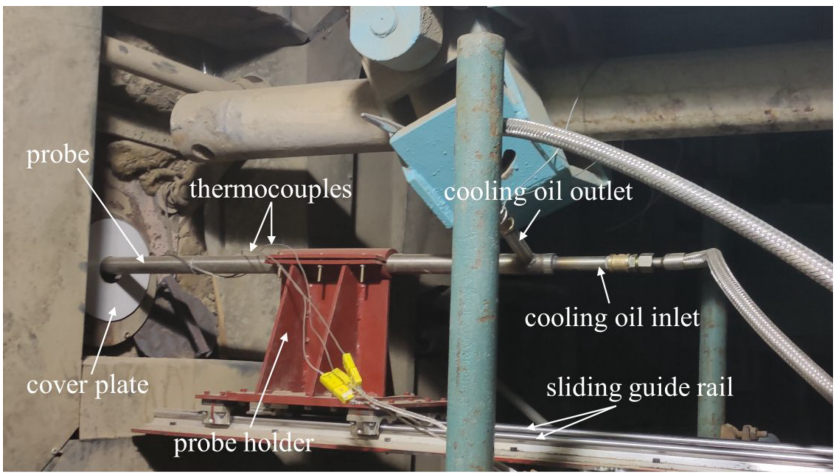

FIGURE 3 Test site picture of the deposition collection system

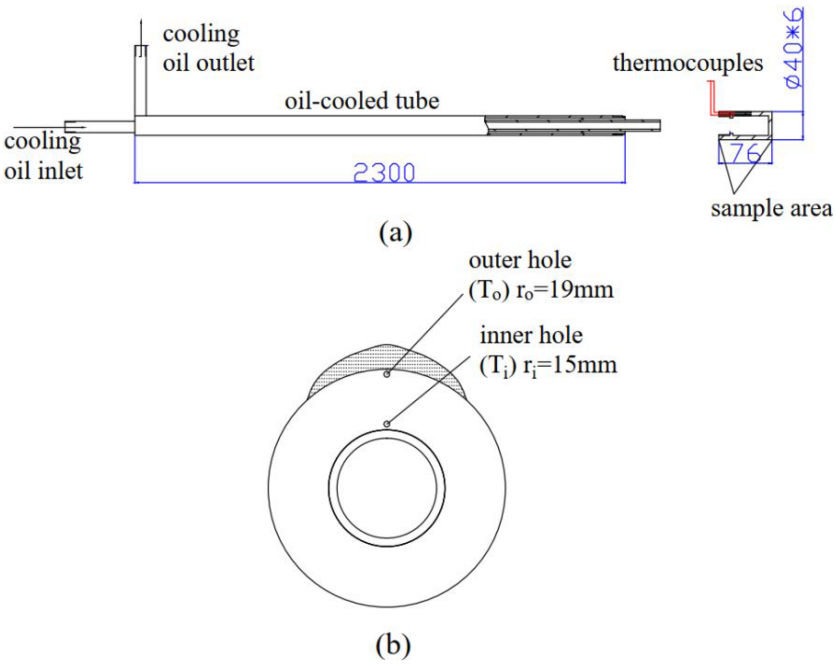

FIGURE 4 (a) Schematic diagram of the probe; (b) probe head cross-sectional view

the coal was loaded in the coal bunker, and then, the mixture was sent into the coal mills. Combustion conditions of the two slag chambers were the same. For HMc condition, both slag chambers burnt HM coal. The average load of the test was 255 MW, and the average smoke temperature of each measuring point is shown in Table 3.

3 | RESULTS AND DISCUSSION

3.1 | The main parameters of the boiler during the tests

During the test, the temperature and pressure values of main steam and reheat steam by every 5 min are shown

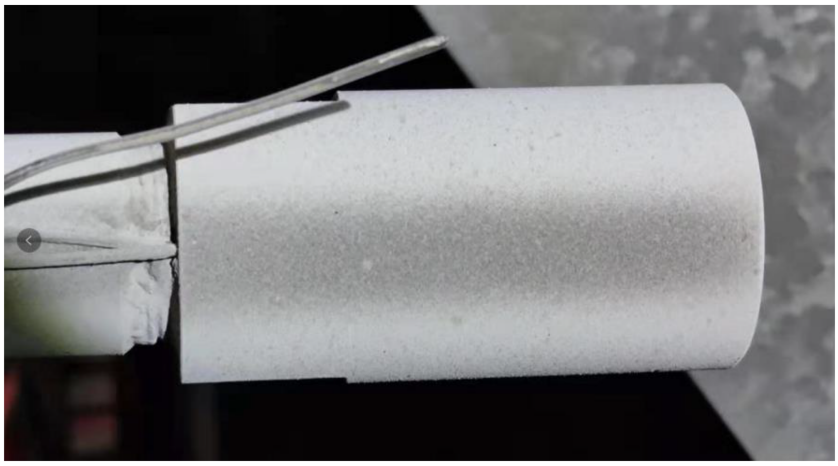

FIGURE 5 Picture of ash deposition on the probe head. (a) Main steam temperature, (b) main steam pressure, (c) Reheat steam temperature, and (d) reheat steam pressure

TABLE 1 Coal properties

	Proximate analysis (wt.%, ad)				Ultimate analysis (wt.%, ad)					Ash fusion temperature (°C)			
	M	A	V	Fc	C	H	O	N	S	DT	ST	HT	FT
SH	15.44	11.23	24.25	49.08	59.75	2.66	8.95	1.61	0.36	1074	1105	1118	1135
HM	11.28	14.45	25.08	49.19	57.82	2.99	10.79	1.85	0.82	1075	1088	1099	1125

TABLE 2 Chemical composition of the coal ash

	SiO_2	Al_2O_3	CaO	Fe_2O_3	SO_3	Na_2O	K_2O	MgO	TiO_2	P_2O_5
SH	31.88	18.73	21.91	10.42	9.77	1.00	1.07	2.91	1.06	0.13
HM	24.08	13.41	17.44	17.90	20.78	2.09	0.83	2.02	0.85	0.12

TABLE 3 Mean flue gas temperature at each measuring point

	SH5	RH2	RH1	ECON
Temperature/°C	835	707	634	388

in Figure 6; the full lines in the figure denote the average temperature and pressure values of main steam and reheat steam whose concrete values are shown in Table 4. From Figure 6 and Table 4, it could be seen that the temperature and pressure of the main steam and reheat steam changed a little. They fluctuated around the average. And the deviations based on SHc condition have been calculated. The main steam temperature deviations under 2.5%Na, 4%Na, and HMc conditions were 0.05%, −0.22%, and 0.03%, and the pressure deviations were −0.59%, −0.23%, and −0.27%, respectively; the temperature deviations of the reheated steam were −0.02%, 0.12%, and −0.03%, and the pressure deviations were −3.93%, 2.52%, and 1.72%. Except for the slightly larger deviation of reheat steam pressure, the deviations of temperature and pressure of main steam and the pressure of reheat steam were almost negligible. Therefore, when the high-alkali coal was burnt in the boiler with slag-tap furnace, it would hardly affect the safe and stable operation of the boiler.

3.2 | Distribution of different elements in various conditions

Table 5 shows the XRF results of samples at each measuring point, fly ash, and liquid slag. Among them, Na_2O and K_2O are marked in bold, which will be discussed in depth next. To more clearly express the changes in the content of different elements, the stacked plots of slag and deposition samples at different positions are drawn, as shown in Figure 7. It could be seen that the main components of each sample were SiO_2, Al_2O_3, CaO, and Fe_2O_3, which accounted for more than 88% of the total weight. The content of Al_2O_3 was almost the same in each sample. The content of Fe_2O_3 in the liquid slag was higher than the content of other measuring positions, especially in the HMc condition. In contrast, the distribution of Ca content showed the opposite trend. Compared with the original ash, the SO_3 content in the measured samples was very low, for most of the S was oxidized into SO_2

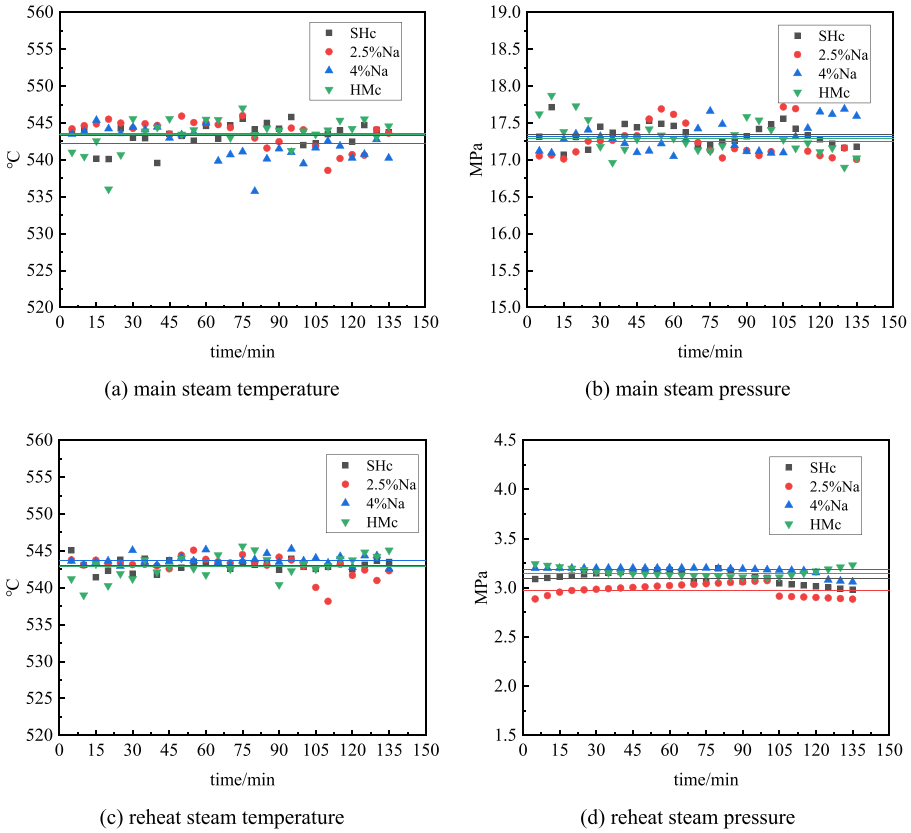

(a) main steam temperature

(b) main steam pressure

(c) reheat steam temperature

(d) reheat steam pressure

FIGURE 6 (a, c) Temperature and (b, d) pressure of main steam and reheat steam

	Main steam		Reheat steam	
	Temperature/°C	Pressure/MPa	Temperature/°C	Pressure/MPa
SHc	543.37	17.35	543.09	3.10
2.5%Na	543.62	17.25	542.96	2.98
4%Na	542.16	17.31	543.77	3.18
HMc	543.55	17.30	542.92	3.15

TABLE 4 Average temperature and pressure of main steam and reheat steam

or SO_3 and entered the flue gas. A small amount of S existed in the ash and liquid slag as compounds.

Figure 8 shows the content curve of Na, K. Figure 8a is the Na content curve. After the pulverized coal entered the slag chamber, it was immediately heated and began to burn. Na element in coal was mainly sublimated directly into Na vapor or released rapidly in the form of Na_2O and NaCl. Part of the Na element combined with Si and Al to form aluminosilicate into the liquid slag in the slag chamber, and the other part directly entered the flue gas. When the flue gas temperature decreases, sulfate aerosols are formed and deposited on the surface of the fly ash.[9,24] The flue gas temperature at the SH5 was about 835°C, where Na mainly existed in sodium vapor. Sodium vapor rapidly condensed once it contacted the low-temperature surface of the probe, resulting in a higher Na content in this position. When the flue gas temperature dropped, Na in the gas phase would be precipitated and adhered to the fly ash. After the fly ash continuously collided on the heat transfer surface, the proportion of fine ash in the fly ash increased in the back section of the flue. The finer ash particles would deposit on the probe head by thermophoresis.[25] Since the Na content in finer ash is higher than in the crude ash,[26] the Na at the later measuring point increased slightly. When the Na content in the fuel increased, the Na content in each sample increased, especially in the flue gas. Under the HMc condition, the Na content curve in the flue gas was close to the 4%Na condition, which might be related to the $(SiO_2 + Al_2O_3)/Na_2O$ ratio. The content of Si and Al was related to the capture and volatilization of Na, and Wang et al.[27] found that the larger the $(SiO_2 + Al_2O_3)/Na_2O$ ratio, the better the capture of

TABLE 5 Chemical composition of each sample

	LS	SH5	RH2	RH1	ECON	Fly ash	LS	SH5	RH2	RH1	ECON	Fly ash
	SHc						2.5%Na					
SiO_2	42.29	36.62	35.53	35.34	35.88	34.69	41.37	36.80	35.40	35.75	35.92	35.76
Al_2O_3	15.99	21.17	20.04	19.41	19.21	19.49	17.14	20.19	18.95	18.70	18.73	18.63
CaO	17.33	22.98	25.25	26.48	26.97	27.36	18.37	23.19	24.27	25.37	25.76	26.13
Fe_2O_3	18.66	10.94	11.81	11.42	10.72	10.90	16.84	10.75	11.95	11.45	11.00	11.19
SO_3	0.15	1.48	1.25	1.16	1.13	1.83	0.10	1.42	1.27	1.09	1.10	1.44
Na_2O	**0.73**	**0.83**	**0.80**	**0.92**	**1.04**	**0.82**	**1.39**	**1.72**	**1.86**	**1.78**	**1.96**	**1.73**
K_2O	**2.04**	**1.49**	**1.36**	**1.40**	**1.54**	**1.64**	**1.87**	**1.45**	**1.45**	**1.49**	**1.56**	**1.82**
MgO	0.70	1.47	1.16	1.04	0.98	0.99	0.86	1.67	1.47	1.59	1.32	1.03
TiO_2	0.96	1.28	1.22	1.22	1.20	1.35	1.01	1.22	1.60	1.30	1.26	1.46
P_2O_5	0.07	0.23	0.21	0.19	0.16	0.25	0.09	0.26	0.25	0.20	0.19	-
	HMc						4%Na					
SiO_2	41.12	35.10	35.59	35.85	35.95	35.99	32.60	30.47	30.02	32.02	33.33	34.17
Al_2O_3	17.55	19.30	18.10	17.85	17.96	18.06	17.32	17.98	17.64	18.31	17.79	19.19
CaO	18.00	23.43	24.23	24.42	25.35	25.07	12.87	26.27	23.23	21.77	23.16	23.26
Fe_2O_3	16.96	11.35	12.04	11.73	11.06	11.28	31.71	13.90	19.36	19.00	15.85	13.44
SO_3	0.09	1.99	1.71	1.96	1.36	1.78	0.28	3.13	2.08	1.70	2.03	2.13
Na_2O	**1.43**	**2.89**	**2.52**	**2.52**	**2.84**	**2.71**	**1.19**	**2.33**	**2.29**	**2.51**	**2.53**	**2.46**
K_2O	**1.89**	**1.56**	**1.61**	**1.66**	**1.65**	**1.85**	**0.97**	**0.79**	**0.66**	**0.73**	**0.91**	**1.27**
MgO	0.84	1.36	1.25	1.12	1.20	0.99	0.96	2.28	2.16	1.83	1.96	1.63
TiO_2	1.00	1.28	1.27	1.22	1.26	1.33	0.95	1.15	1.28	1.05	1.13	1.30
P_2O_5	0.08	0.18	0.15	0.15	0.14	0.21	0.12	0.24	0.17	0.15	0.20	0.31

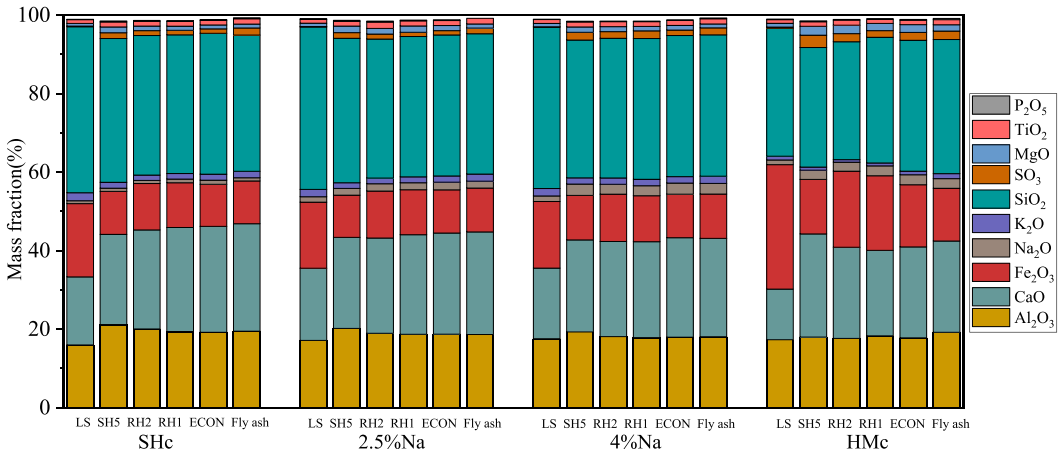

FIGURE 7 Stacking diagram of oxide composition of each sample. (a) Na and (b) K

Na. The $(SiO_2 + Al_2O_3)/Na_2O$ ratios in 4%Na and HMc conditions were 12.27 and 17.93, respectively, which were relatively close, so their curves were also close. And the ratio of HMc condition was slightly larger than 4%Na, resulting in the HMc curve below 4%Na. Figure 8b is the K content curve. The K content in the liquid slag was greater than that in the flue gas. At the same time, it could be seen that the increase of the Na content in the fuel would slightly increase the K content in the sample. As the K content in HMc was relatively small, the K content in the sample was lower than in the SHc condition.

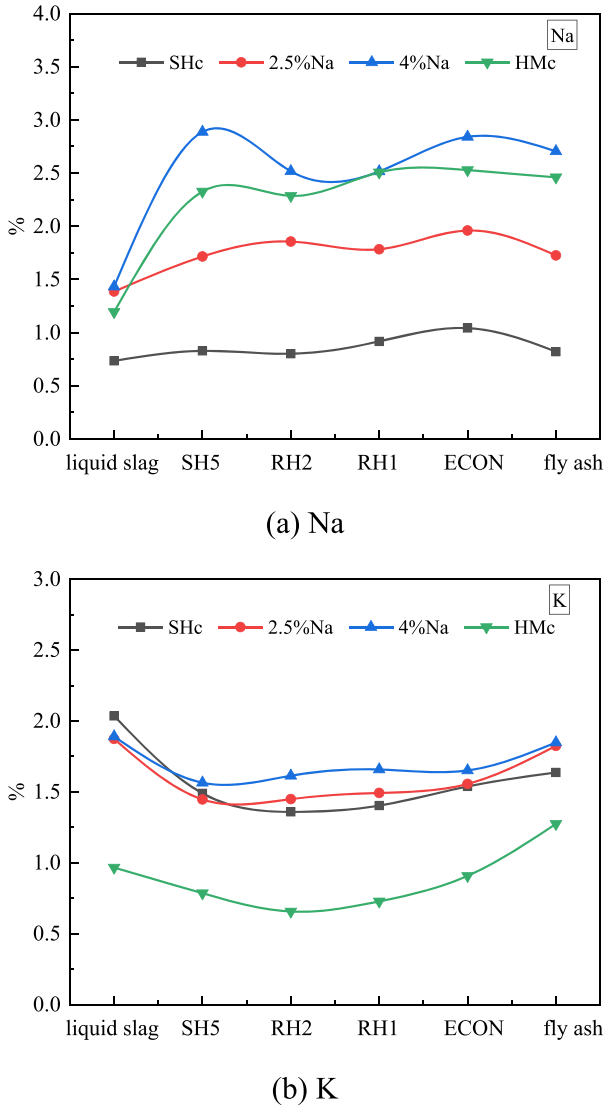

FIGURE 8 (a) Na and (b) K content of each measuring point in various conditions

3.3 | The effects of adding Na_2CO_3 on the migration properties of elements

The molten liquid slag could capture alkali metals. When the molten liquid slag was in contact with coal particles burning in the flue gas, an interfacial reaction occurred on the contact interface. Liquid slag would capture Na and K in the coal and make them free in the Si-Al system of the liquid slag. Stable high melting point compounds like $Na_4Ca(SO_4)_3 \cdot 2H_2O$, $NaCa_2HSi_3O_9$, and $KCaAl_3Si_3O_{12} \cdot 5H_2O$[20] would be formed, thereby reducing the alkali metal content in the flue gas. Adding Na_2CO_3 would affect the capture ability of liquid slag. Based on the SHc condition, relative change ratios of Na content (R_{Na}) under 2.5%Na and 4%Na conditions could be calculated according to formula 1.

$$R_{Na} = \frac{Na_{i,j} - Na_i}{Na_i} \times 100\%, \quad (1)$$

where Na_i denotes the Na content of SHc condition; $Na_{i,j}$ denotes the Na content of the experimental groups; i denotes the sampling position (the value of i is LS, SH5, RH2, RH1, ECON, and fly ash.); j denotes test conditions (the value of j is 2.5%Na, 4%Na.). Similarly, R_K can be defined. The results are shown in Figure 9.

Figure 9a displays the relative change ratio of Na content. For 2.5%Na and 4%Na conditions, generally speaking, when the Na content in coal ash was increased by 150% and 300%, the Na content in the samples of liquid slag, SH5, RH2, RH1, ECON, and fly ash should also be increased to the corresponding ratio. However, due to many lower temperature heat transfer surfaces in the boiler, a large amount of Na would condense on the heat transfer surface, resulting in the increase of Na content in the samples not reaching 150% and 300%. After adding Na_2CO_3, the Na in coal ash would increase. Under 2.5%Na and 4%Na conditions, the R_{Na} of liquid slag was 88.75% and 95.14%, respectively, which were far less than 150% and 300%. This illustrated that when the other chemical components in the coal ash remained unchanged, only the Na content increased and the capture ability of the liquid slag would increase to some extent. But this improvement was limited. More Na got into the flue gas. Simultaneously, as could be seen that the difference between R_{Na} of 4%Na and 2.5%Na was only 6.39%, indicating that the capture ability of liquid slag on Na was close to saturation before the proportion of Na in the coal ash increased by 150%. So the boiler with slag-tap furnace may not perform as well when burning coals with higher alkali metal content. However, compared with a dry bottom boiler, the advantages of the boiler with slag-tap furnace mainly lie in the larger share of liquid slag and the smaller share of fly ash. It can capture more alkali metals by increasing the share of liquid slag. At the same time, when burning coal with higher alkali metal content, it is possible to capture more alkali metal by increasing the Al and Si contents by adding kaolin.

Figure 9b shows the relative change ratio of K content. For the 2.5%Na and 4%Na conditions, the R_K at each measurement position increased slightly. The R_K in the liquid slag decreases slightly because the increase of Na content in the fuel weakened the capture ability of liquid slag to K; it tended to capture Na. Therefore, part of K ran into the flue gas.

Figure 10 displays the Si, Fe, Al, and Ca content of each measuring point. The addition of Na_2CO_3 had little effect on the migration of Si and Fe elements but

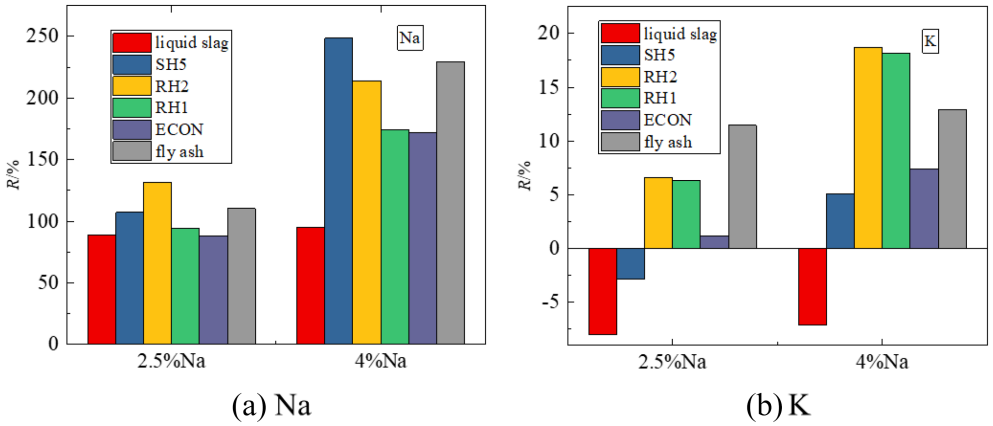

FIGURE 9 Relative change ratios of (a) Na and (b) K content of each measuring point in various conditions relative to the blank group

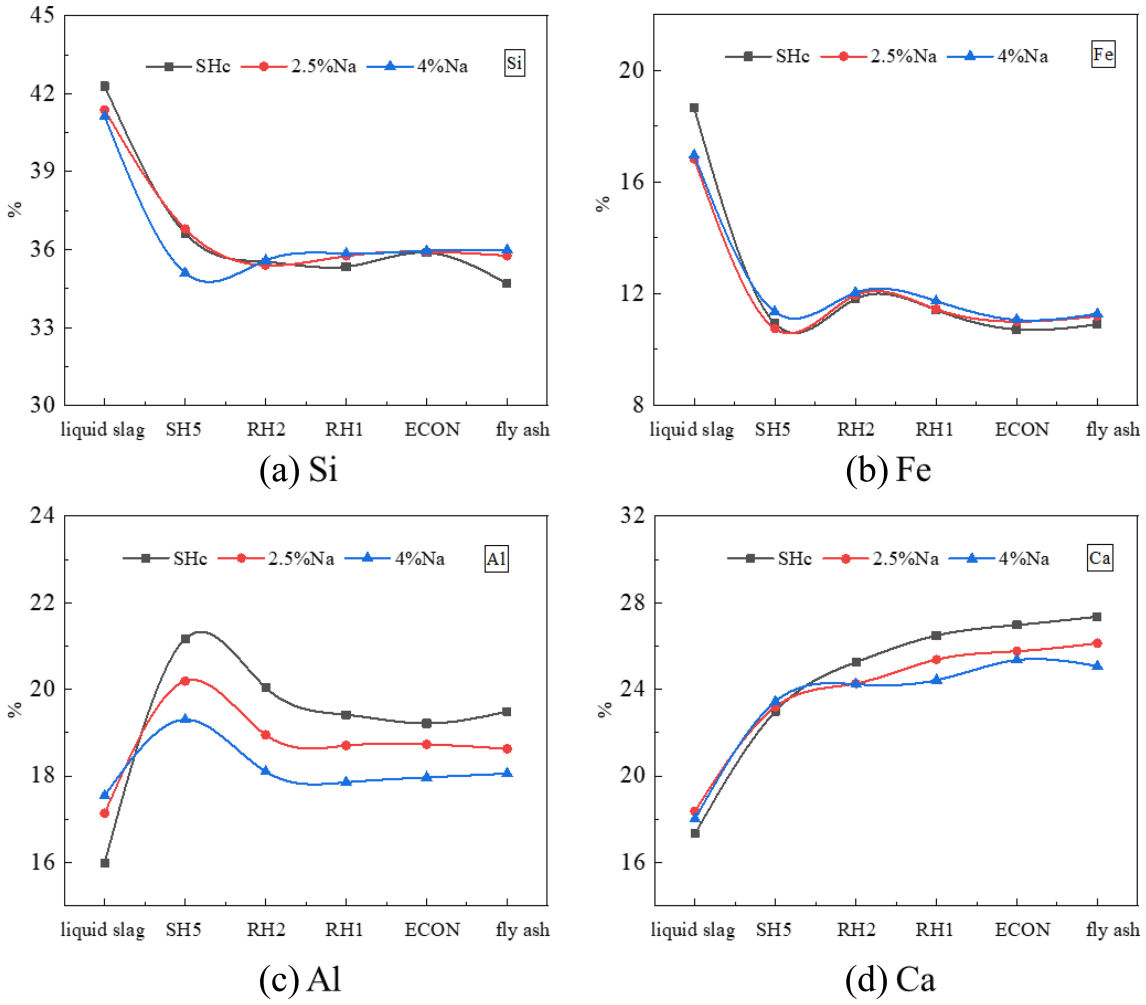

FIGURE 10 (a) Si, (b) Fe, (c) Al, and (d) Ca content of each measuring point

had a greater effect on the migration of Al and Ca elements. After adding Na_2CO_3, the content of Si and Fe in the liquid slag decreased (Figure 10a,b), while the content of Al and Ca increased (Figure 10c,d). In the flue gas, the content of Si and Fe did not change significantly, and the content of Al and Ca decreased with the addition of Na_2CO_3. The more Na_2CO_3 was added, the more Al and Ca content decreased, indicating that when Na_2CO_3 was co-fired with coal particles at a high temperature in the slag chamber, the fixed Na in the liquid slag generated more high-melting Na-Al-Ca compounds.

3.4 | Microstructure of slag and deposition

Figure 11 shows the appearance of slag under four conditions. The solidified liquid slag was black and glassy, with many pores on the surface and inside, and the number of small pores was more than the number of large pores. The liquid slag under the four conditions had little difference in appearance. Break up the slag and analyze the microstructure of the slag and deposition. The SEM results are shown in Figure 12. The surface of the liquid slag was very flat and smooth, with a lot of micropores inside under all conditions. The micropores were analyzed by EDS. And the results are shown in Table 6. Among them, the content of Na is marked in bold and compare. An interesting phenomenon was found that the Na content inside the micropores was higher than outside. Because the temperature of the molten liquid slag was very high, Na was gasified into vapor in some places where Na was enriched. Before this part of the Na vapor could be released to the surface of the liquid slag, the liquid slag was cooled and solidified, so the Na vapor was cooled on the surface of the micropores, leading to a higher Na content inside. From the picture of the ash

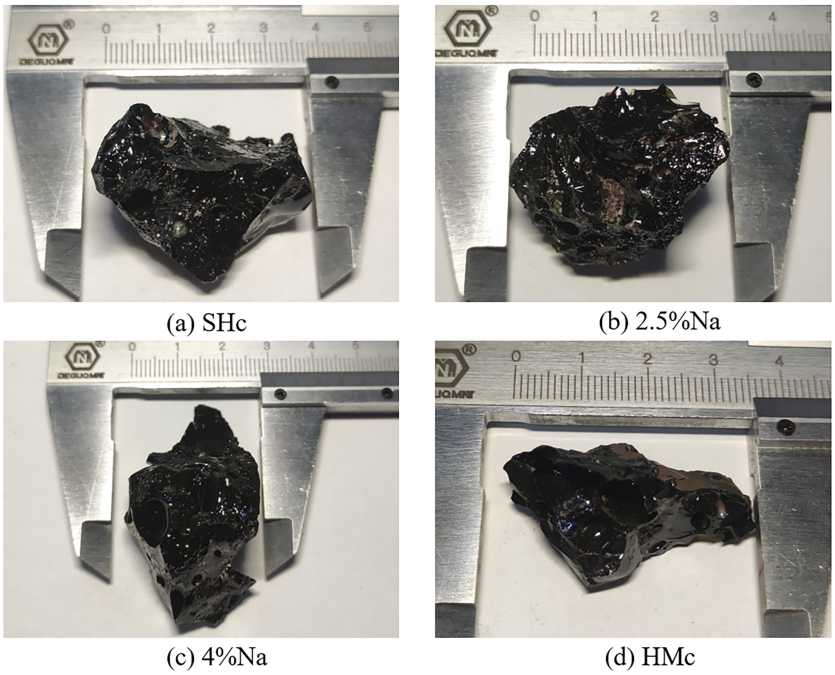

FIGURE 11 The appearance of slag under SHc, 2.5%Na, 4%Na and HMc conditions

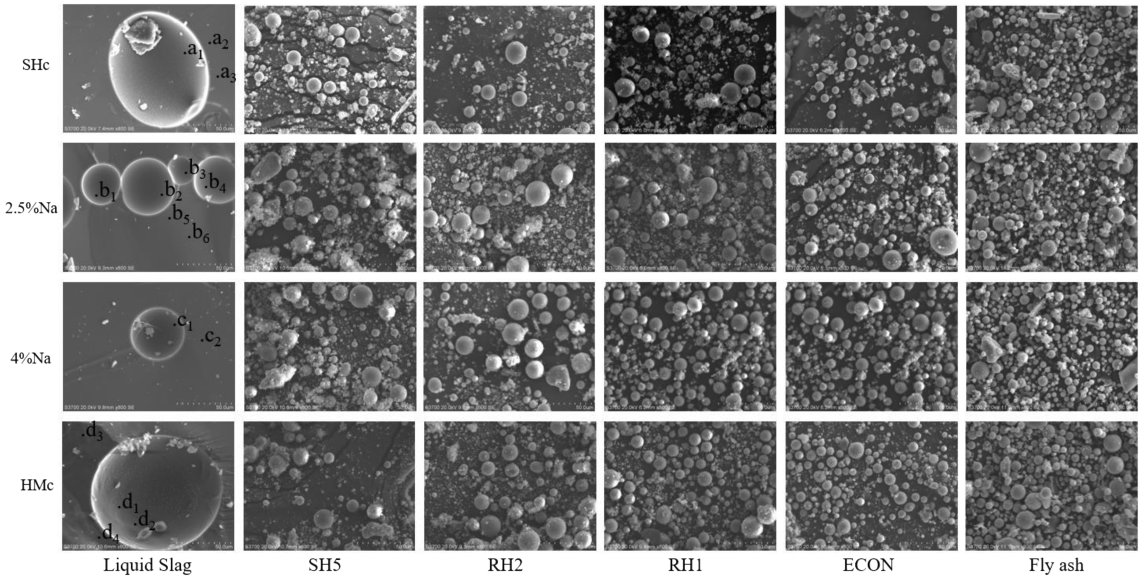

FIGURE 12 The microstructure of slag and deposition

TABLE 6 The EDS results of spots in slag

	Point	Na	Ca	Al	Si	K	Mg	Fe	O
SHc	a_1	**0.89**	3.72	3.46	11.48	0.51	0	19.91	38.7
	a_2	**0.67**	8.47	7.08	22.12	1.1	0.38	7.54	38.63
	a_3	**0.63**	8.59	7.08	22.79	1.21	0.38	8.21	36.79
2.5%Na	b_1	**0.98**	5.04	5.68	20.19	1.26	0.23	7.52	48.19
	b_2	**0.69**	7.07	5.51	21.01	1.71	0.27	11.24	39.99
	b_3	**0.92**	4.55	5.61	19.79	1.03	0.31	5.84	49.38
	b_4	**0.98**	4.5	5.69	20.34	1.16	0.28	6.18	49.65
	b_5	**0.81**	7.88	6.52	22.39	1.36	0.43	7.45	39.29
	b_6	**0.80**	4.55	5.61	19.79	1.03	0.31	5.84	49.38
4%Na	c_1	**2.14**	6.76	5.28	10.72	0.65	0	24.28	39.65
	c_2	**2.04**	6.23	7.24	21.2	0.96	0.44	5.25	44.24
HMc	d_1	**1.07**	6.17	5.67	16.95	0.78	0.61	14.04	39.01
	d_2	**1.2**	4.05	5.15	14.28	0.48	0.56	9.42	50.51
	d_3	**0.86**	7.01	6.9	18.15	0.65	0.6	14.04	38.31
	d_4	**0.95**	5.24	6.53	16.44	0.52	0.7	10.78	46.54

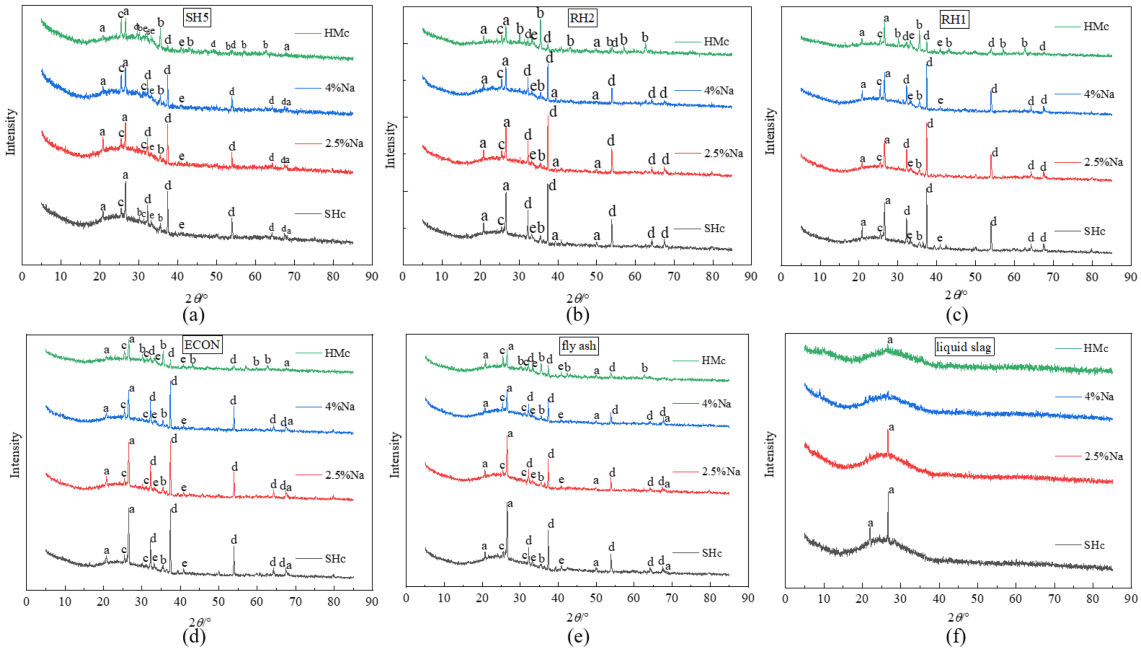

FIGURE 13 XRD patterns of samples at different measuring points under various conditions: (a) SiO_2 (quartz); (b) $MgFe_2O_4$ (Magnesioferrite); (c) $CaSO_4$ (anhydrite); (d) CaO (lime); (e) $CaSiO_4$ (calcium silicate)

sample, ash particles with the roughened surface could be found at SH5 and RH2, for sodium vapor and ash particles adhered to the probe head at low temperature, and sodium vapor acted as a binder between the ash particles and the probe head, leading to a roughened surface. When the temperature dropped to 600°C, the sodium vapor was condensed entirely. So the surface of the ash particles at RH1, ECON, and fly ash was smooth. Due to multiple collisions with the heat transfer surface, bigger particles were broken along the flue gas direction, and more tiny particles appeared in the ash samples.

3.5 | Mineralogy of slag and deposition

X-ray diffraction (XRD) analysis was conducted to understand all samples' mineralogy for four conditions. XRD patterns are displayed in Figure 13. Figure 13a–e shows

the XRD patterns of ash samples collected at SH5, RH2, RH1, ECON, and fly ash. The mineralogical analysis results of the ash samples were relatively similar. The main minerals were quartz (SiO_2), magnesioferrite ($MgFe_2O_4$), anhydrite ($CaSO_4$), lime (CaO), and calcium silicate ($CaSiO_4$). The temperature gradually decreased along the flue gas direction. The minerals in the ash sample that did not change for the coal particles had been completely burned, and the temperature was not high enough to cause further changes in the crystal structure. At the same time, it was found that the added Na_2CO_3 did not affect on the minerals of the ash sample because after entering the furnace, Na_2CO_3 was heated and decomposed into Na_2O and CO_2. Most sodium was quickly gasified into sodium vapor and entered the flue gas, and the remaining Na was converted into aluminosilicate and entered into the liquid slag. Figure 13f shows the XRD analysis curve of liquid slag. The curve fluctuated greatly and was not as smooth as other samples, indicating that the slag had a lower degree of crystallinity. The slag was mainly composed of glassy amorphous material, so there was no obvious diffraction peak. Because the slag with a high Si/Al ratio had a low crystallization tendency, the viscosity increased gradually as the temperature decreased, closer to the characteristics of glassy slag.[28] HM coal contained more Fe_2O_3, as shown in Table 2, so $MgFe_2O_4$ in ash sample under HMc condition had better crystallinity and higher diffraction peaks.

4 | CONCLUSIONS

This work explored the possibility of fully burning high-alkali coal in a 300 MW boiler with slag-tap furnace by carrying out a Na_2CO_3 blending test and a fully burning high-alkali coal test. A self-made probe was used to collect the deposition before the heat transfer surfaces in the boiler. Meanwhile, the liquid slag and the fly ash at the tail of the flue were collected. By analyzing the chemical composition and material composition of the samples, the conclusions could be drawn as follows:

1. During the test, the boiler operates stably; the temperature and pressure of main steam and the temperature of reheat steam change little, only the pressure of reheat steam changes a little larger.
2. Due to changes in temperature and ash particle size, the Na content in the flue gas tends to decrease from SH5 to RH2 and increase from RH2 to ECON. The increase of the Na content in the fuel will greatly increase the Na content in the flue gas and, at the same time, will raise the K content slightly. The change of alkali metal in HMc is mainly related to the high $(SiO_2 + Al_2O_3)/Na_2O$ ratio and the low K content in HM coal ash.
3. After adding Na_2CO_3, the Na content of the experimental group is much higher than that of the blank group, which is related to the Na content in the fuel and the capture ability of the liquid slag. When the Na content in coal ash is increased by 150% and 300%, the R_{Na} of liquid slag is 88.75% and 95.14%. Before the Na content in SH coal ash is increased by 150%, the Na capture capacity of the liquid slag has reached saturation. The added Na_2CO_3 makes the Al and Ca elements migrate to the liquid slag to form a high melting point Na-Al-Ca compound.
4. Liquid slag has a rich pore structure outside and inside. And the tiny pores in the slag have a feature that Na content in the pore is higher than out. Due to the condensation of sodium vapor, ash particles at SH5 and RH2 have a rough surface. More tiny particles appear along the flue gas direction in the ash samples.
5. Except for liquid slag, the samples at each measuring point mainly include Quartz, Magnesioferrite, Anhydrite, Lime, and $CaSiO_4$. The addition of Na_2CO_3 scarcely affects the mineral composition and the intensity of diffraction peaks. The high Fe content in HM coal ash leads to a strong diffraction peak of Magnesioferrite.

ACKNOWLEDGEMENT

This work was supported by the National Key Research & Development Program of China (2018YFB0604104).

ORCID

Hao Zhou https://orcid.org/0000-0001-9779-7703

REFERENCES

1. China Electricity Council. *Annual Development Report of China's Power Industry 2021*. Beijing: China Building Materials Press; 2021.
2. Zhou JB, Zhuang XG, Alastuey A, Querol X, Li J. Geochemistry and mineralogy of coal in the recently explored Zhundong large coal field in the Junggar basin, Xinjiang province, China. *Int J Coal Geol*. 2010;82(1–2):51-67. doi:10.1016/j.coal.2009.12.015
3. Wu SM. Xin jiang Ha Mi coal chemical industry development in environmental issues environment and development. *Northern Environment*. 2011;23(9):13-21.
4. Zhang SY, Chen C, Shi DZ, et al. Situation of combustion utilization of high sodium coal. *CSEE*. 2013;33(5):1-12.
5. Li GD, Li SQ, Huang Q. Fine particulate formation and ash deposition during pulverized coal combustion of high-sodium lignite in a down-fired furnace. *Fuel*. 2015;143:430-437. doi:10.1016/j.fuel.2014.11.067
6. Wang XB, Xu ZX, Wei B, et al. The ash deposition mechanism in boilers burning Zhundong coal with high contents of sodium

and calcium: A study from ash evaporating to condensing. *Appl Therm Eng*. 2015;80:150-159. doi:10.1016/j.applthermaleng.2015.01.051

7. Niu YQ, Tan HZ, Hui S. Ash-related issues during biomass combustion: alkali-induced slagging, silicat melt-induced slagging (ash fusion), agglomeration, corrosion, ash utilization, and related countermeasures. *Prog Energy Combust Sci*. 2016;52:1-61. doi:10.1016/j.pecs.2015.09.003
8. Zhou H, Xing YJ, Zhou MX. Effects of modified kaolin adsorbents on sodium adsorption efficiency and ash fusion characteristics during Zhundong coal combustion. *J Energy Inst*. 2021;97:203-212. doi:10.1016/j.joei.2021.04.017
9. Wang XB, Xu ZX, Wei B. The ash deposition mechanism in boilers burning Zhundong coal with high contents of sodium and calcium: A study from ash evaporating to condensing. *Appl Therm Eng*. 2015;80:150-159. doi:10.1016/j.applthermaleng.2015.01.051
10. Li GY, Wang CA, Wang PQ, et al. Ash deposition and alkali metal migration during Zhundong high-alkali coal gasification. *Energy Procedia*. 2017;105:1350-1355. doi:10.1016/j.egypro.2017.03.497
11. Dou BL, Shen WQ, Gao JS, Sha X. Adsorption of alkali metal vapor from high-temperature coal-derived gas by solid sorbents. *Fuel Process Technol*. 2003;82(1):51-60. doi:10.1016/S0378-3820(03)00027-4
12. Dai BQ, Wu X, de Girolamo AD, Cashion J, Zhang L. Inhibition of lignite ash slagging and fouling upon the use of a silica-based additive in an industrial pulverised coal-fired boiler: Part 2. Speciation of iron in ash deposits and separation of magnetite and ferrite. *Fuel*. 2015;139:733-745. doi:10.1016/j.fuel.2014.06.075
13. Low F, Girolamo AD, Wu X, Dai B, Zhang L. Inhibition of lignite ash slagging and fouling upon the use of a silica-based additive in an industrial pulverised coal-fired boiler: Part 3 - Partitioning of trace elements. *Fuel*. 2015;139:746-756. doi:10.1016/j.fuel.2014.09.015
14. Zhang T, Li ZS, Hu F, Huang X, Liu Z. Correlation of sodium releasing and mineral transformation characteristics with ash composition of typical high-alkali coals. *Fuel Process Technol*. 2021;224:107035. doi:10.1016/j.fuproc.2021.107035
15. Nielsen HP, Frandsen FJ, Dam-Johansen K, Baxter LL. The implications of chlorine-associated corrosion on the operation of biomass-fired boilers. *Prog Energy Combust Sci*. 2000;26(3):283-298. doi:10.1016/S0360-1285(00)00003-4
16. Mayoral MC, Aadres JM, Belzunce J, Andrés JM, Higuera V. Study of sulphidation and chlorination on oxidized SS310and plasma-sprayed Ni-Cr coatings as simulation of hot corrosion in fouling and slagging in combustion. *Corros Sci*. 2006;48(6):1319-1336. doi:10.1016/j.corsci.2005.06.004
17. Li LM. Design and application of 350 MW supercritical boiler burning Zhundongcoal[J]. *Power System Engineering*. 2014;(2):39-41.
18. Zhao YG, Wang ZC, Yao H, et al. Key parameters design for 600 MW unit boiler firing 100% Zhundong high alkali coal. *Therm Power Gen*. 2020;49(6):111-117.
19. Lan DH, Fan JJ, Zhang ZX, Hu XL, Chen SL. Experimental study on combustion of high alkali coal in horizontal liquid slag cyclone furnace. *Clean Coal Technol*. 2020;26(4):119-126.
20. Li MQ, Fan JJ, Zhang ZX, Wu XJ. Mechanism study on liquid slag capture of alkali metal. *J Combust Sci Technol*. 2017;23(5):429-435.
21. Zhou GQ, Zhang XL, Yao W, Zhang S. Experimental study on combustion and fouling characteristics of Zhundong high sodium coal in liquid slagging cyclone furnace. *Therm Power Gen*. 2018;47(11):40-45.
22. Qiu JY. Experimental study at cold state on horizontal cyclone slag-tapping equipment for high-alkali coal. *Boil Technol*. 2018;49(4):1-5.
23. Tang MT, Zhang ZK, Ma ZZ, Wang J, Yang JC, Shen BX. Effect of sodium compounds on the migration of Na and S during the slag-tap of high-alkali coal. *J Hebei Univ Technol*. 2022;51(1):54-60.
24. Li GY, Wang CA, Yan Y, Jin X, Liu Y, Che D. Release and transformation of sodium during combustion of Zhundong coals. *J Energy Inst*. 2016;89(1):48-56. doi:10.1016/j.joei.2015.01.011
25. Baxter LL. Ash deposition during biomass and coal combustion: A mechanistic approach. *Biomass Bioenergy*. 1993;4(2):85-102. doi:10.1016/0961-9534(93)90031-X
26. Chen J, Jiao FC, Dong ZB, et al. Effect of kaolin on ash partitioning during combustion of a low-rank coal in O_2/CO_2 atmosphere. *Fuel*. 2018;222:538-543. doi:10.1016/j.fuel.2018.02.191
27. Wang JR, Chen FM, Zhao B, Li X, Qin L. Volatilisation and transformation behavior of sodium species at high temperature and its influence on ash fusion temperatures. *Fuel Process Technol*. 2017;155:209-215. doi:10.1016/j.fuproc.2016.06.009
28. Chen X, Kong L, Bai J, et al. The key for sodium-rich coal utilization in entrained flow gasifier: the role of sodium on slag viscosity-temperature behavior at high temperatures. *Appl Energy*. 2017;206:1241-1249. doi:10.1016/j.apenergy.2017.10.020

How to cite this article: Ni Y, Hu S, Meng H, et al. Experimental research on fully burning high-alkali coal in a 300 MW boiler with slag-tap furnace. *Asia-Pac J Chem Eng*. 2022;17(5):e2807. doi:10.1002/apj.2807